

Spin wave excitation in yttrium iron garnet films with micron-sized antennas

Y. V. Khivintsev, Y. A. Filimonov, and S. A. Nikitov

Citation: [Applied Physics Letters](#) **106**, 052407 (2015); doi: 10.1063/1.4907626

View online: <http://dx.doi.org/10.1063/1.4907626>

View Table of Contents: <http://scitation.aip.org/content/aip/journal/apl/106/5?ver=pdfcov>

Published by the [AIP Publishing](#)

Articles you may be interested in

[Spin waves in micro-structured yttrium iron garnet nanometer-thick films](#)

J. Appl. Phys. **117**, 17D128 (2015); 10.1063/1.4916027

[Spin-wave excitation and propagation in microstructured waveguides of yttrium iron garnet/Pt bilayers](#)

Appl. Phys. Lett. **104**, 012402 (2014); 10.1063/1.4861343

[Single antidot as a passive way to create caustic spin-wave beams in yttrium iron garnet films](#)

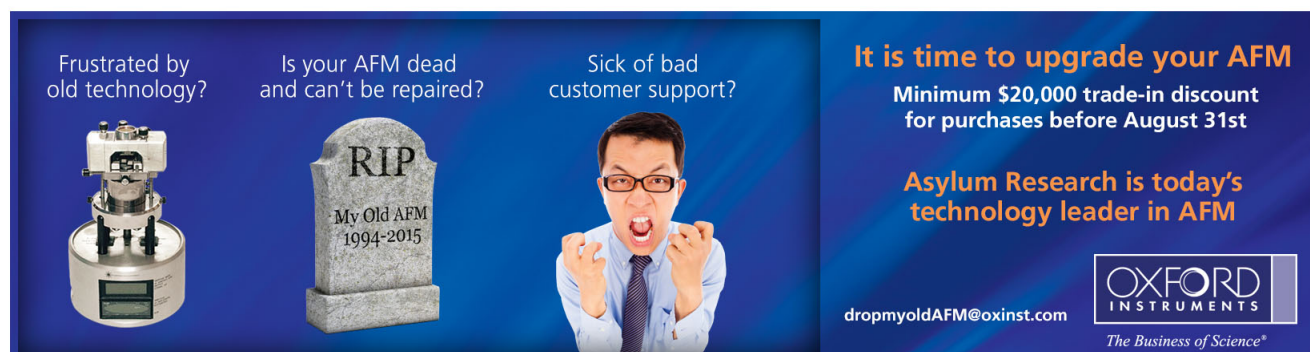
Appl. Phys. Lett. **102**, 102409 (2013); 10.1063/1.4795293

[Amplification of spin waves in yttrium iron garnet films through the spin Hall effect](#)

Appl. Phys. Lett. **99**, 192511 (2011); 10.1063/1.3660586

[Double-wave-front reversal of dipole-exchange spin waves in yttrium-iron garnet films](#)

J. Appl. Phys. **98**, 074908 (2005); 10.1063/1.2077842

The advertisement is set against a dark blue background with a subtle wave pattern. It is divided into three main sections. The first section on the left shows a photograph of an old, bulky AFM instrument. The middle section features a grey tombstone with the inscription 'RIP My Old AFM 1994-2015'. The third section on the right shows a man in a white shirt and tie, looking frustrated with his hands raised. To the right of these images, white text reads: 'Frustrated by old technology?', 'Is your AFM dead and can't be repaired?', and 'Sick of bad customer support?'. On the far right, a large white box contains the text: 'It is time to upgrade your AFM', 'Minimum \$20,000 trade-in discount for purchases before August 31st', and 'Asylum Research is today's technology leader in AFM'. At the bottom right, the Oxford Instruments logo is displayed, consisting of the word 'OXFORD' in a large, bold, sans-serif font above the word 'INSTRUMENTS' in a smaller, bold, sans-serif font, all enclosed in a white rectangular border. Below the logo, the text 'The Business of Science®' is written in a small, italicized font. At the bottom left of the advertisement, the email address 'dropmyoldAFM@oxinst.com' is provided.

Spin wave excitation in yttrium iron garnet films with micron-sized antennas

Y. V. Khivintsev,^{1,2,a)} Y. A. Filimonov,^{1,2} and S. A. Nikitov^{2,3}

¹Kotel'nikov IRE RAS, Saratov Branch, 410019 Saratov, Russia

²Chernyshevsky Saratov State University, 410012 Saratov, Russia

³Kotel'nikov IRE RAS, 125009 Moscow, Russia

(Received 18 December 2014; accepted 25 January 2015; published online 5 February 2015)

In this paper, we explore spin waves excitation in monolithic structures based on yttrium iron garnet (YIG) films with micro-sized antennas. Samples based on plain and patterned YIG film were fabricated and tested for tangential bias field geometries. We observed spin wave excitation and propagation with wave numbers up to 3.5×10^4 rad/cm. The corresponding wavelength is thus shorter more than by one order of magnitude compared to previous experiments with such films. For the sample with a periodic array of nanotrenches, we observed the effect of the shape anisotropy resulting in the shift of the spin wave propagation band in comparison to the unpatterned YIG film. Our results are very promising for the exploitation of short spin waves in YIG and provide great opportunity for significant miniaturization of YIG film based microwave devices. © 2015 AIP Publishing LLC. [<http://dx.doi.org/10.1063/1.4907626>]

For a long time yttrium iron garnet (YIG), films remain as one of the most attracting materials for the investigation of propagating spin waves (SW) and the development of SW devices for microwave signal processing, due to extremely low magnetic damping compared to other magnetic thin film materials.^{1,2} The SWs properties in YIG films are utilized for variety of the microwave devices such as isolators, circulators, tunable filters, and phase shifters.¹ At this moment, the miniaturization of such devices and their integration with planar on-chip microwave circuits remain very important challenges. Recently, there have been reports on the fabrication of quite high quality YIG films on non-orienting substrates³ that can potentially help in the integration of SW devices with other types of solid state microwave devices. In this paper, we report on the generation and propagation of SWs in YIG films that are much shorter than in previous works. The results provide great opportunities for the miniaturization of SW devices based on YIG films.

In most of the microwave experiments on YIG films as well as in SW microwave devices, the dipole part of the SW dispersion relation is utilized. In this case, SWs—usually called magnetostatic waves (MSWs)—are excited and detected by antennas fabricated on a dielectric substrate (usually planar transmission line or coplanar waveguide antennas) that is placed in contact with the YIG film.^{2,4,5} The typical width of the antennas that defines the minimal wavelength is around $50 \mu\text{m}$ that usually allows for effective excitation/detection of SWs with the wave numbers below 10^3 rad/cm. The shortest spin waves observed in experiments using this approach had wave numbers of about 3×10^3 rad/cm.⁵

One of the possible ways for the operation of shorter SWs was already demonstrated by Eshbach⁶ who used the so called Schlomann's mechanism⁷ based on the wavelength conversion in a strongly non-uniform internal magnetic field in order to excite SWs with the wave numbers of about

10^5 rad/cm in a YIG disk. Later, a similar mechanism was developed for the SW excitation in epitaxial YIG films using a non-uniform distribution of the effective magnetization across the film thickness.⁸ However, this approach based on utilization of the non-uniform magnetic state is quite complicated in a sense of practical applications for regular YIG films.

Another possible approach for the excitation and detection of shorter SWs in YIG films lies in the direct integration and reduction of the lateral dimensions of the antennas. During the last years, micron-sized antennas have been extensively used in experiments on SWs in ferromagnetic metallic films,^{9–12} where the propagation length was much smaller than in YIG and the application of such antennas was crucial. The goal of our work is to explore such micron-sized antenna structures for the excitation of surface and bulk SWs in YIG films.

In our experiments, we used a $0.5 \mu\text{m}$ thick monocrystalline YIG film grown on gadolinium gallium garnet substrate (GGG) by liquid phase epitaxy. Micron-sized antennas for excitation and detection of the SWs were fabricated directly on the top of the YIG film by lift-off technique using photolithography and thermal evaporation of gold and an adhesion layer through a resist mask. The antennas were in the form of a shorted $300 \mu\text{m}$ long coplanar waveguide (CPW) with $2 \mu\text{m}$ wide gold signal and ground lines separated by

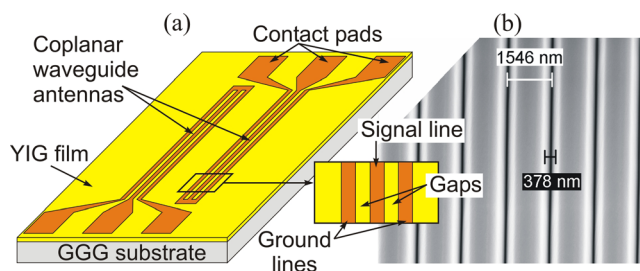


FIG. 1. Geometry of the samples: (a) sketch and (b) SEM image of the patterned YIG film. Dark lines indicate the trenches etched by a focused ion beam.

^{a)}Electronic mail: khivintsev@gmail.com

1.6 μm wide gaps—see Fig. 1(a). Open ends of the CPWs had contact pads for using microwave probes.

Three samples with antennas were fabricated on one-and-the-same chip. The first two samples had different separations of 12 and 24 μm between the inner conductors of input and output antennas. In the third sample, the antennas were separated by 12 μm and fabricated on a prepatterned YIG film incorporating a periodic array of nanotrenches. The trenches were 300 μm long and had a period of 1.5 μm (Fig. 1(b)). We used focused ion beam etching with Ga ions to generate trenches with a width of about 400 nm. The antennas were collinear with the trenches.

Microwave measurements were done using a vector network analyzer along with a microwave probe station. Scattering parameters were measured as a function of the frequency at different bias magnetic fields. The external in-plane bias field was applied along or perpendicular to the antennas that corresponded to the excitation of a magnetostatic surface wave (MSSW) and magnetostatic backward volume wave (MSBVW), respectively.¹³ Measurements were carried out at input power of -30 dBm that was below the threshold power at which effects of the SWs parametric instability would arise leading to an increased SW attenuation. Before measurements, the on-wafer TRL (Thru, Reflect, Line) calibration was applied in order to avoid effects of microwave cables and probes.

For both MSSW and MSBVW geometries, we observed two transmission bands corresponding to the first and second spatial harmonics of the CPW antennas—see Fig. 2. In the case of the antennas separated by 24 μm , the minimal insertion loss for the transmission band corresponding to the first spatial harmonic was about -18 dB and -28 dB for MSSW and MSBVW, respectively, at the cross-talk level below -50 dB. The transmission band corresponding to the second spatial harmonic was more pronounced for MSBVWs which probably related to the fact that the group velocity in this case did not drop down so dramatically with increased wave number compared to the MSSWs. As one could expect, the transmission was reciprocal in the case of the MSBVW (Fig. 2(c)) and strongly nonreciprocal in the case of the MSSW

(Fig. 2(a)), with a difference in transmission parameters for opposite propagation directions of up to 20 dB.

Using phase characteristics of the transmission parameters (Figs. 2(b) and 2(d)), the experimental dispersion of the waves was calculated from the following relation:¹⁴

$$k(f) = \varphi_{\text{SW}}(f)/L, \quad (1)$$

where k and f are the wave number and frequency of the SW, respectively; φ_{SW} is the relative phase shift due to the SW propagation with respect to the SW frequency f at $k=0$ (minimal frequency of the transmission bands in the case of the MSSW and maximal—in the case of MSBVW); L is the propagation length taken as the distance between inner conductors of the antennas.¹² It is difficult to define the frequency corresponding to the $k=0$ SW taking into account that the CPW antennas have significant filtering properties and do not effectively excite and detect long SWs (with small wave numbers). To describe also further uncertainties in the phase shift (through, e.g., a delay of the signal in antennas, effect of the cross talk, remaining discrepancies for the calibration), we used an additional relation given by

$$\varphi_{\text{M}}(f) = \varphi_{\text{SW}}(f) + \varphi_0, \quad (2)$$

where φ_{M} is the total (measured) phase shift and φ_0 is the unknown phase shift that was used in the calculations as a fitting parameter in order to get the best matching with theoretically expected dispersion accordingly to equations obtained by Damon and Eshbach.¹³ In order to reduce the effect of the crosstalk signal, the calculations were done point by point only in the frequency range where the SW signal was above the cross talk level by more than 10 dB (Figs. 2(a) and 2(c)). Outside this range, only the points corresponding to jumps in the measured amplitude and phase characteristics related with the 2π shift in the SW phase¹⁴ were used in calculations. The best matching between the experiment and theory was found when we used the bias field as an additional fitting parameter. The comparison between theory (with typical for YIG saturation magnetization of 1.75 kG) and experimental data is presented in Fig. 3. The fitted bias field value deviated

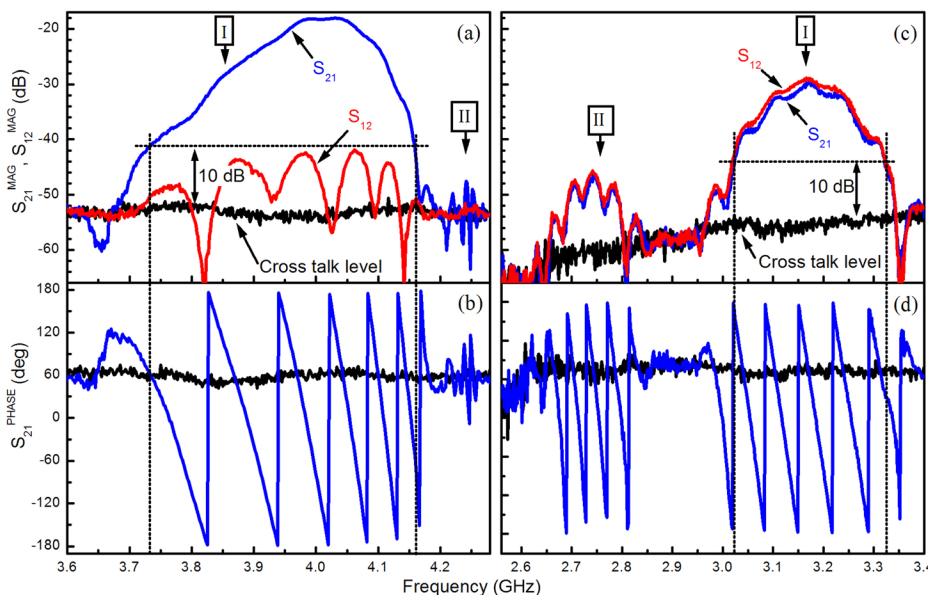


FIG. 2. S_{21} magnitude (a) and (c) and phase (b) and (d) vs frequency for MSSW (a) and (b) and MSBVW (c) and (d). Bias field is 620 Oe for (a) and (b) and 651 Oe for (c) and (d). Distance between antennas is 24 μm .

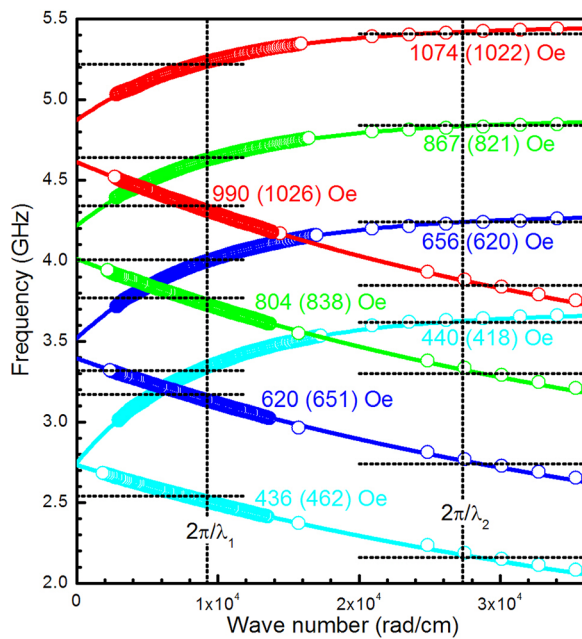


FIG. 3. Dispersion for MSSW and MSBVW for various bias fields. Dots show experimental data, and solid lines represent results of theoretical calculations using. Numbers next to data are magnetic fields used as a fitting parameter and actual bias fields indicated in brackets. Horizontal and vertical dotted lines indicate the frequencies corresponding to the maximum in the SW transmission bands and the wave numbers corresponding to the averaged values of λ_1 and λ_2 , respectively.

by less than 6% from the nominal bias field value. The discrepancy is attributed to the effect of magnetic anisotropy that was not taken into account in calculations and the different positions of the field sensor and the sample in the experiment. We note that we performed further calculations for dispersion relations taking into account the exchange interaction¹⁵ (with typical for YIG exchange constant of 4×10^{-9} Oe·cm² and assuming unpinned spins at the surface) but did not find a perceptible effect of the exchange interaction in the considered wave number range.

Using transmission characteristics as shown in Fig. 2 and the results of Fig. 3, we determined the frequencies and wave numbers corresponding to the maximum in the SW transmission bands. Averaged values of the wavelength corresponding to the first and second SW propagation bands for all bias fields were $\lambda_1 = 6.8 \pm 0.6$ μ m and $\lambda_2 = 2.3 \pm 0.2$ μ m, respectively. These values are in good agreement with the geometry of the CPW antennas taking into account that the maximum antenna efficiency for the first and second spatial harmonics corresponds to $\lambda/2$ and $3\lambda/2$ between the gaps in the CPW antennas. This confirms the correctness of the obtained dispersion data.

From Fig. 3, one can see that in our experiment, we were able to observe SW excitation and propagation in a quite wide range of wave numbers, i.e., from about 10^3 to 3.5×10^4 rad/cm. The last number indicates more than one order expansion to shorter spin waves in comparison to MSW experiments utilizing traditional contact structure excitation/detection system.

The samples based on the plain YIG film with a shorter SW propagation length of 12 μ m showed similar results (Fig. 4). Insertion loss was about the same as for the structure with

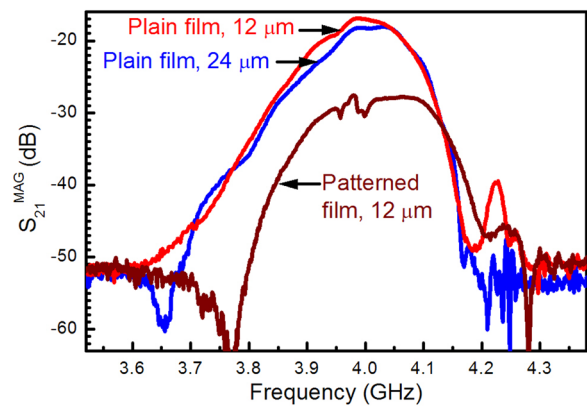


FIG. 4. S_{21} magnitude vs frequency in MSSW geometry at bias field of 620 Oe for different samples: the plain film with 24 μ m between the antennas, the plain film with 12 μ m between the antennas, and the patterned film with 12 μ m between the antennas.

24 μ m between the antennas, indicating that in both cases, it is mostly attributed to the excitation/detection loss but not to the propagation loss. The sample with the patterned YIG film showed an insertion loss increased by about 10 dB. At the same time, the SW transmission band was shifted to larger frequencies compared to the unpatterned samples. This is attributed to the shape anisotropy effect. We note that we did not observe any evidence of the formation of the Bragg stop bands in the transmission characteristics which are typical for patterned periodical structures based on YIG.^{2,4,15} This was because the period of our patterned structure corresponded to Bragg resonances at frequencies where the antennas did not efficiently excite and detect SWs (between the observed transmission bands corresponding to the first and second spatial harmonics of the antennas). Still, for some applied fields, the propagation band for the patterned YIG film exhibited one or two small absorption features—see peaks in the range of 3.9–4 GHz in Fig. 4. We presume that this feature resulted from the interaction of the MSSW with the exchange modes.^{5,15} For uniform films with unpinned spins at the surfaces, such interaction should be negligible but patterning can lead to so-called dynamic pinning effect that could force this interaction.¹⁶

As a general conclusion, we reported short-wavelength SWs in monolithic structures based on YIG films that were excited with integrated micron-sized antennas. We find such structures very promising for the miniaturization of YIG film based microwave devices. We showed that direct writing of nanotrenches in YIG film with a focussed ion beam allows one to locally modify the transmission characteristics of SWs.

We note that the results on observation of so short spin waves in monolithic structures based on YIG films with micro-sized antennas was originally reported at conferences.¹⁷ Recently, there have also been published similar results¹⁸ but for structures based on ultra-thin YIG films fabricated by the pulsed laser deposition which exhibit much smaller propagation length and group velocities.

This work was supported by European Community's Seventh Framework Programme (Grant No. 247556), Grant of the Government of the Russian Federation for supporting

scientific research projects supervised by leading scientists at Russian institutions of higher education (Project No. 11.G34.31.0030), Russian Foundation for Basic Research (Grant Nos. 13-07-00941, 13-07-12421, and 14-07-00896). Also, we wish to thank R. Huber, T. Schwarze, and D. Grundler from Technical University of Munich for help with the samples fabrication and measurements as well as for helpful discussion on this manuscript.

- ¹D. B. Chrisey, P. C. Dorsey, J. D. Adam, and H. Buhay, *Thin Films* **28**, 319 (2001).
- ²A. A. Serga, A. V. Chumak, and B. Hillebrands, *J. Phys. D: Appl. Phys.* **43**, 264002 (2010).
- ³Y. Sun, Y. Y. Song, and M. Wu, *Appl. Phys. Lett.* **101**, 082405 (2012).
- ⁴E. N. Beginin, Yu. A. Filimonov, E. S. Pavlov, S. L. Vysotskii, and S. A. Nikitov, *Appl. Phys. Lett.* **100**, 252412 (2012).
- ⁵A. S. Andreev, Yu. V. Gulyaev, P. E. Zil'berman, V. B. Kravchenko, A. V. Lugovskoi, Yu. F. Ogrin, A. G. Temiryazev, and L. M. Filimonova, *Sov. Phys. JETP* **59**, 586 (1984).
- ⁶J. R. Eshbach, *J. Appl. Phys.* **34**, 1298 (1963).
- ⁷E. Schloemann, *Advances in Quantum Electronics* (Columbia University Press, New York, 1961).

- ⁸P. E. Zil'berman, A. G. Temiryazev, and M. P. Tikhomirova, *Phys.-Usp.* **38**, 1173 (1995).
- ⁹V. E. Demidov, M. P. Kostylev, K. Rott, J. Munchenberger, G. Reiss, and S. O. Demokritov, *Appl. Phys. Lett.* **99**, 082507 (2011).
- ¹⁰L. Fallarino, M. Madami, G. Duerr, D. Grundler, G. Gubbiotti, S. Tacchi, and G. Carlotti, *IEEE Trans. Magn.* **49**, 1033 (2013).
- ¹¹R. Huber, M. Krawczyk, T. Schwarze, H. Yu, G. Duerr, S. Albert, and D. Grundler, *Appl. Phys. Lett.* **102**, 012403 (2013).
- ¹²C. S. Chang, M. Kostylev, E. Ivanov, J. Ding, and A. O. Adeyeye, *Appl. Phys. Lett.* **104**, 032408 (2014).
- ¹³R. W. Damon and J. R. Eshbach, *J. Phys. Chem. Solids* **19**, 308 (1961).
- ¹⁴W. Schilz, Philips Res. Rep. **28**, 50 (1973).
- ¹⁵R. E. De Wames and T. Wolfram, *J. Appl. Phys.* **41**, 987 (1970).
- ¹⁶S. L. Vysotskii, S. A. Nikitov, and Y. A. Filimonov, *J. Exp. Theor. Phys.* **101**, 547 (2005).
- ¹⁷Y. V. Khivintsev, R. Huber, T. Schwarze, D. Grundler, Y. A. Filimonov, and S. A. Nikitov, in *International Symposium on Spin Waves 2013, Abstract book* (Ioffe Physical-Technical Institute, St. Petersburg, Russia, 2013), p. 67; Y. Khivintsev, V. Sakharov, R. Huber, T. Schwarze, D. Grundler, Y. Filimonov, and S. Nikitov, in *IEEE International Magnetic Conference "Intermag Europe 2014," Digest book* (IEEE, 2014), pp. 1120–1121.
- ¹⁸H. Yu, O. d'Allivy Kelly, V. Cros, R. Bernard, P. Bortolotti, A. Anane, F. Brandl, R. Huber, I. Stasinopoulos, and D. Grundler, *Sci. Rep.* **4**, 6848 (2014).